Image-guided optical spectroscopy provides molecular-specific information *in vivo*: MRI-guided spectroscopy of breast cancer hemoglobin, water, and scatterer size

Colin M. Carpenter, Brian W. Pogue, Shudong Jiang, Hamid Dehghani, Xin Wang, and Keith D. Paulsen
Thayer School of Engineering, Dartmouth College, Hanover, New Hampshire 03755, USA

Wendy A. Wells
Department of Pathology, Dartmouth Medical School, Lebanon, New Hampshire 03756, USA

Jorge Forero, Christine Kogel, John B. Weaver, and Steven P. Poplack
Department of Diagnostic Radiology, Dartmouth Medical School, Lebanon, New Hampshire 03756, USA

Peter A. Kaufman
Department of Medicine, Dartmouth Medical School, Lebanon, New Hampshire 03756, USA

Received December 19, 2006; accepted January 9, 2007;
posted January 18, 2007 (Doc. ID 78274); published March 19, 2007

A multimodality instrument that integrated optical or near-infrared spectroscopy into a magnetic resonance imaging (MRI) breast coil was used to perform a pilot study of image-guided spectroscopy on cancerous breast tissue. These results are believed to be the first multiwavelength spectroscopic images of breast cancer using MRI-guided constraints, and they show the cancer tumor to have high hemoglobin and water values, decreased oxygen saturation, and increased subcellular granularity. The use of frequency-domain diffuse tomography methods at many wavelengths provides the spectroscopy required for recovering maps of absorbers and scattering spectra, but the integration with MRI allows these data to be recovered on an image field that preserves high resolution and fuses the two data sets together. Integration of molecular spectroscopy into standard clinical MRI can be achieved with this approach to spectral tomography.

OCIS codes: 170.0110, 170.3880.

Medical imaging systems have largely been focused on revealing anatomy at increasing spatial resolution. However, growing interest has developed in discerning the functional biologic properties of tissue, particularly cancers. The downside of most imaging modalities that report functional information is low spatial resolution. Functional imaging can be combined with higher-resolution anatomic imaging to associate function and structure (PET/CT being the most significant clinical combination). In recent years the concept of image-guided regional spectroscopy has emerged,[1,2] and there have been systematic technical advances reported in the literature in key clinical trials.[3,4] Here, we report that tomographic diffuse near-infrared spectroscopy (NIRS) has been combined with magnetic resonance imaging (MRl) in the setting of breast cancer imaging, with the critical step that the MR image is used as the template upon which spectroscopy is localized, to create spatially resolved functional images of breast cancer progression/regression. The use of full spectroscopy and recovery of accurate chromophore and scattering related particle size values is a key step in the pathway of determining the biomedical utility of MRI-guided NIRS.

Near-infrared spectroscopy (NIRS) has a 30 year history of being used to assess tissue hemoglobin oxygen saturation, molecular tagging *in vivo*, elastic scattering, and *in vivo* luminescence in experimental studies. This is largely done without high resolution, and while there has been some focus on developing better imaging capabilities, the ability to achieve high-resolution imaging with NIRS is fundamentally limited. Integration of NIRS using multiple point measurements with image guidance and constraints allows the recovery of spatially mapped regions of these parameters, where the spatial information comes from another imaging modality, and the spectral information is provided by mapping the NIRS light propagation onto the image through diffuse image reconstruction.[1–3,5–7]

In this study, dynamic contrast enhanced T1 MRI and NIRS were acquired simultaneously using the system shown in Figs. 1(a)–1(c). Images of the breast pre-and-post contrast injection were obtained to create the views shown in Figs. 1(d) and 1(f). For the case study presented, the enhancing region in the breast was targeted to generate localized spectral information. NIRS measurements across the entire breast from 16 source and detector locations were recorded to provide the overlapping information needed for tomographic spectral recovery of functional data,[6] with acquisition requiring 15 min per plane and being completed both before and after the contrast in-

0146-9592/07/080933-3/$15.00

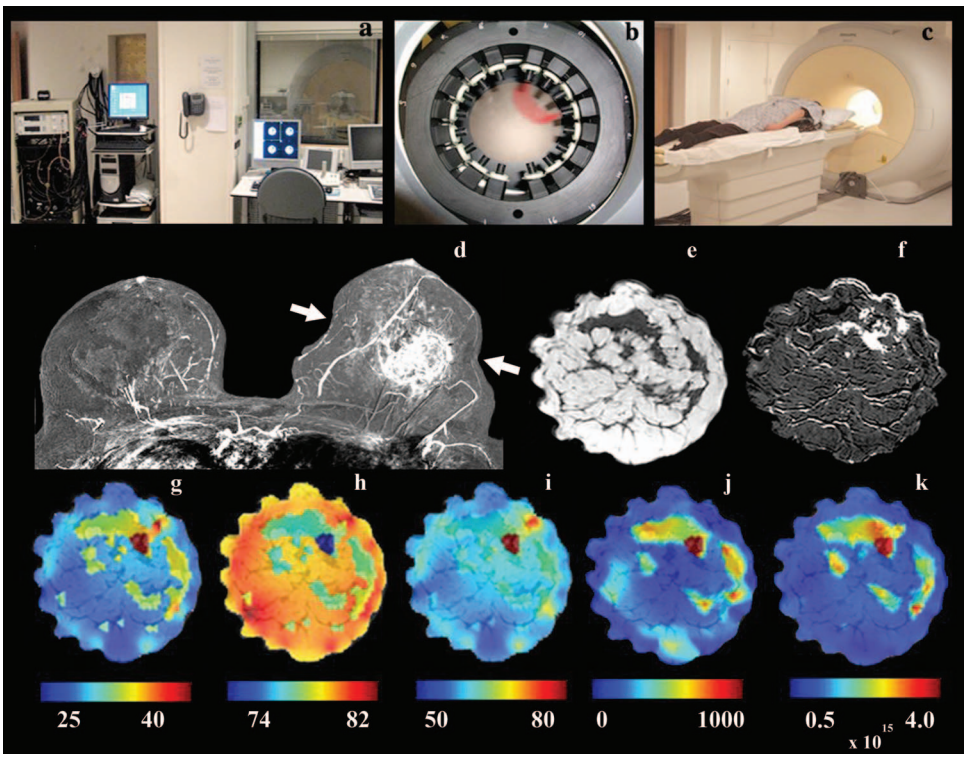

Fig. 1. Photographs (top row) of a, control systems for NIRS and MRI; b, NIR interface placed inside the MRI breast coil with a diffuse light path between one source and detector fiber indicated in red; c, a patient lying prone on the breast coil on the MRI bed. The second row shows d, axial T_1 MR images with dynamic contrast enhancement in a maximal intensity projection showing both entire breasts to scan where the tumor was. The arrows denote the plane of the NIR imaging array. Image e is a coronal T_1 view prior to injection, and f is a subtraction image of post–pre injection, both in the plane of the tumor. Reconstructed images from NIRS (bottom row) include; g, hemoglobin (units of micromolar); h, oxygen saturation (%); i, water fraction (units of %); j, effective scatterer particle size (units of nm); k, scatterer particle number density.

jection. Structural information (e.g., adipose, fibroglandular, and suspected tumor tissues) was segmented from the MR to estimate the localized NIRS concentration parameters through an inverse spectral solution process that incorporates the spatial information as constraints.[5] The technique provides bulk concentrations of the primary tissue absorbers, including oxy-hemoglobin, deoxy-hemoglobin, and water. Additionally, it is known that the scattering spectrum is related to the scatterer particle size and number density distributions in tissue, and the spectral fit estimates the effective average values of these quantities in the different tissues.[7]

NIRS images are created using spectroscopy data measured through the breast, along with an optical transport-based model with an iterative inverse reconstruction algorithm. The optical fluence data are obtained by surrounding the breast with 16 fiber-optic bundles and transmitting light from each fiber one at a time and detecting at all other fibers in parallel. This provides 16 sources and 15 detectors, for a total of 240 data points, with each data set then repeated at all five discrete wavelengths from 660 up to 850 nm, as described in Ref. 7. The light is intensity modulated at 100 MHz frequency to allow measurement of the amplitude and phase shift of the signal. At these high frequencies, the phase shift provides a critical measurement of the optical path length through the tissue. Light transport through scattering media such as tissue is modeled at each wavelength with a diffusion approximation to the radiative transport equation,[8] as shown below,

$$-\nabla \cdot D(r)\,\nabla\,\Phi(r,\omega) + \left[\mu_a(r) + \frac{i\omega}{c}\right]\Phi(r,\omega) = S(r,\omega), \tag{1}$$

where $\Phi(r,\omega)$ is the optical fluence at position r and modulation frequency ω. The diffusion coefficient is $D = 1/[3(\mu_a + \mu_s')]$, where μ_a is the absorption coefficient and μ_s' is the reduced scattering coefficient. The isotropic source term is $S(r,\omega)$.

The inverse problem was solved directly for the physiological parameters by minimizing the L2 norm of the differences between the model and the data, as well as smoothing out unrealistic magnitudes of these parameters. We also included a smoothing operator within each MR defined region to better guide the reconstruction. This method was developed previously.[5] The inversion minimized is shown below,

$$\min_{\kappa,\mu_a}\{\|\Phi_{\text{meas}} - \Phi_{\text{calc}}\| + \|L(\mu - \mu_0)\|\}, \tag{2}$$

where Φ_{meas} is the data, Φ_{calc} is the modeled data, μ are the physiological parameters, and this first half of the equation is simply what is minimized in most image reconstruction procedures. The difference is in the second term, where L is a Laplacian-type smoothing operator that links pixels in the image within a

given tissue volume to be smoothed but allows discontinuous changes between different types of tissue.

The structure of L is created from the MRI images, segmenting the tissue into distinct regions based upon assumed physiological differences. T1-weighted MR images of the breast were taken pre-and-post Gd enhancement. A postcontrast image in the plane of the optical fibers was then segmented by region into adipose, fibroglandular, and tumor tissue. These were input into the inverse algorithm and defined the regions within L to smooth. The reconstruction uses spectral constraints implied by the known spectra of hemoglobin, oxyhemoglobin, water, and scattering to recover all concentrations at once using the multiwavelength data.[8–10] Images are then displayed superimposed on the MR image.

This case report involved a 29 year woman with a 2 cm infiltrating ductal carcinoma, located mediocaudally in the left breast. The imaging results indicate that the tumor had increased total hemoglobin, decreased oxygen saturation, and increased water content, as shown in Fig. 1(d). The fibroglandular regions have approximately 35 micromolar hemoglobin, and the tumor has 45 micromolar value. The water level in the tumor is 85%, whereas the background tissues are nearer to 65%. The oxygen saturation of the tumor is decreased to 72%, compared with a background fibroglandular tissue of 76%. These changes are all consistent with a higher vascularity and poor drainage of the tumor tissue, with a slightly increased oxygen demand as compared with the supply, and are similar to values previously reported.[6] What has been less studied is the role that elastic scattering can play in characterizing a tumor tissue, and in previous studies the scatter has been shown to have a complex relationship between normal and diseased tissues.[6] Here the tumor region has increased scatter density and effective scatterer size. The increased density of scatterers is an indication of increased granularity in the tumor due to intracellular organelles and extracellular matrix materials on the size scale between 10 and 1000 nm, as indicated by the color-bar scale in Fig. 1(j).

The study demonstrates that NIRS can be added to MRI of specific tissue volumes to quantify their absorption and scattering. Additionally, quantification of contrast agents for absorption or fluorescence is possible. The methods and materials used to achieve this imaging can be directly applied to a range of molecular imaging problems, where the spatial information is obtained through the MR, CT, or ultrasound image and the spectral molecular information is mapped onto this through NIRS.

Correspondence to Brian Pogue at pogue@dartmouth.edu or Colin Carpenter at colin.carpenter@dartmouth.edu.

References

1. R. L. Barbour, H. L. Graber, J. Chang, S. S. Barbour, P. C. Koo, and R. Aronson, IEEE Comput. Sci. Eng. **2**, 63 (1995).
2. B. W. Pogue, T. O. McBride, C. Nwaigwe, U. L. Osterberg, J. F. Dunn, and K. D. Paulsen, Proc. SPIE **3597**, 484 (1999).
3. V. Ntziachristos, A. G. Yodh, M. Schnall, and B. Chance, Proc. Natl. Acad. Sci. U.S.A. **97**, 2767 (2000).
4. R. Choe, A. Corlu, K. Lee, T. Durduran, S. D. Konecky, M. Grosicka-Koptyra, S. R. Arridge, B. J. Czerniecki, D. L. Fraker, A. DeMichele, B. Chance, M. A. Rosen, and A. G. Yodh, Med. Phys. **32**, 1128 (2005).
5. B. Brooksby, S. Jiang, H. Dehghani, B. W. Pogue, K. D. Paulsen, J. B. Weaver, C. Kogel, and S. P. Poplack, J. Biomed. Opt. **10**, 051504 (2005).
6. B. Brooksby, B. W. Pogue, S. Jiang, H. Dehghani, S. Srinivasan, C. Kogel, T. Tosteson, J. B. Weaver, S. P. Poplack, and K. D. Paulsen, Proc. Natl. Acad. Sci. U.S.A. **103**, 8828 (2006).
7. X. Wang, B. W. Pogue, S. Jiang, H. Dehghani, X. Song, S. Srinivasan, B. A. Brooksby, K. D. Paulsen, C. Kogel, A. P. Poplack, and W. A. Wells, J. Biomed. Opt. **11**, 041106 (2006).
8. A. Li, Q. Zhang, J. P. Culver, E. L. Miller, and D. A. Boas, Opt. Lett. **29**, 256 (2004).
9. S. Srinivasan, B. W. Pogue, S. Jiang, H. Dehghani, C. Kogel, S. Soho, J. G. Chambers, T. D. Tosteson, S. P. Poplack, and K. D. Paulsen, Proc. Natl. Acad. Sci. U.S.A. **100**, 12349 (2003).
10. S. Srinivasan, B. W. Pogue, S. Jiang, H. Dehghani, and K. D. Paulsen, Appl. Opt. **44**, 1858 (2004).